

Relating Pore Hydrophilicity with Vapour Adsorption Capacity in a Series of Amino Acid based Metal Organic Frameworks

Tanay Kundu, Subash Chandra Sahoo, Rahul Banerjee*

*Physical/Materials Chemistry Division, CSIR-National Chemical Laboratory, Dr. Homi Bhabha Road,
Pune-411008, India.*

E-mail: r.banerjee@ncl.res.in Fax: + 91-20-25902636; Tel: + 91-20-25902535

Supporting Information

CONTENT

Section S1. Detailed synthetic procedure of ligand and MOF with IR spectrum	3-5
Section S2. Single crystal X-ray diffraction data collection, structure solution and refinement procedure, crystallographic figures.	6-12
Section S3. Variable Temperature Powder X-Ray Diffraction study (VT-PXRD) of ThrZnOAc.	13
Section S4. TGA data and the thermal stability of the ThrZnOAc.	14

Section S1. Detailed synthetic procedures of ligands and MOFs with IR spectrum:

Materials and general methods. All reagents were commercially available and used as received from Sigma Aldrich. Single crystal data were collected on Bruker SMART APEX three circle diffractometer equipped with a CCD area detector and operated at 1500 W power (50 kV, 30 mA) to generate Mo K α radiation ($\lambda=0.71073\text{\AA}$). The incident X -ray beam was focused and monochromated using Bruker Excalibur Gobel mirror optics. Crystals of all MOFs reported in the paper was mounted on nylon CryoLoop (Hampton Research) with Paraton-N (Hampton Research). Powder X-ray diffraction (PXRD) patterns were recorded on a Phillips PANalytical diffractometer for Cu K α radiation ($\lambda = 1.5406 \text{ \AA}$), with a scan speed of 2° min^{-1} with a step size of 0.02° in 2θ . Fourier transform infrared (FT-IR) spectra were taken on a Bruker Optics ALPHA-E spectrometer with a universal Zn-Se ATR (attenuated total reflection) accessory in the $600\text{-}4000 \text{ cm}^{-1}$ region or using a Diamond ATR (Golden Gate). Thermogravimetric experiments (TGA) were carried out in the temperature range of $25\text{-}800 \text{ }^\circ\text{C}$ on a SDT Q600 TG-DTA analyzer under N $_2$ atmosphere at a heating rate of $8 \text{ }^\circ\text{C min}^{-1}$. All low pressure water adsorption experiments (up to 1 bar) were performed on the *Quantachrome* Autosorb-iQ-MP automatic volumetric instrument. NMR data were taken in Bruker 200 MHz NMR spectrometer.

Synthesis:

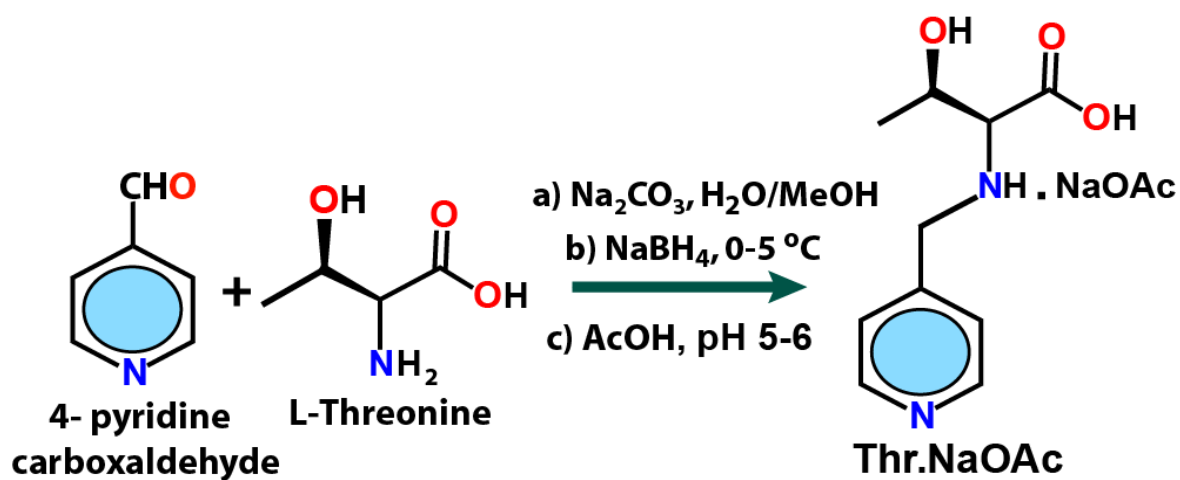


Figure S1: Schematic representation of the ligand synthesis (Thr.NaOAc).

IR Absorption spectrum:

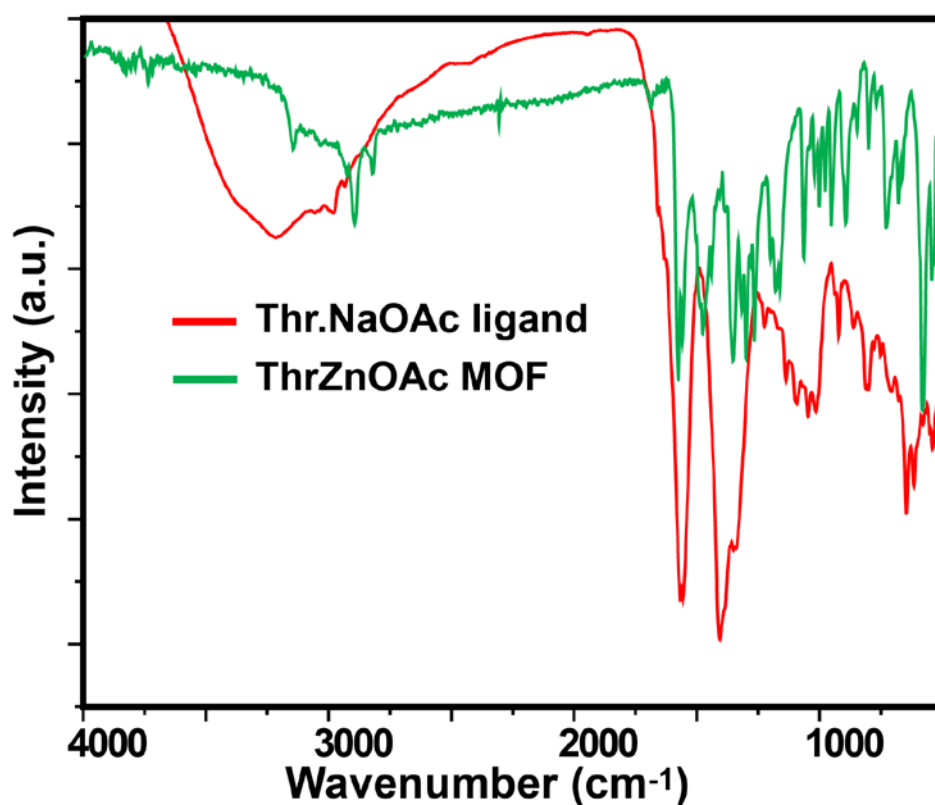


Figure S2. IR Absorption spectrum of Thr.NaOAc ligand (red) and ThrZnOAc MOF (green).

PXRD Pattern of the MOF:

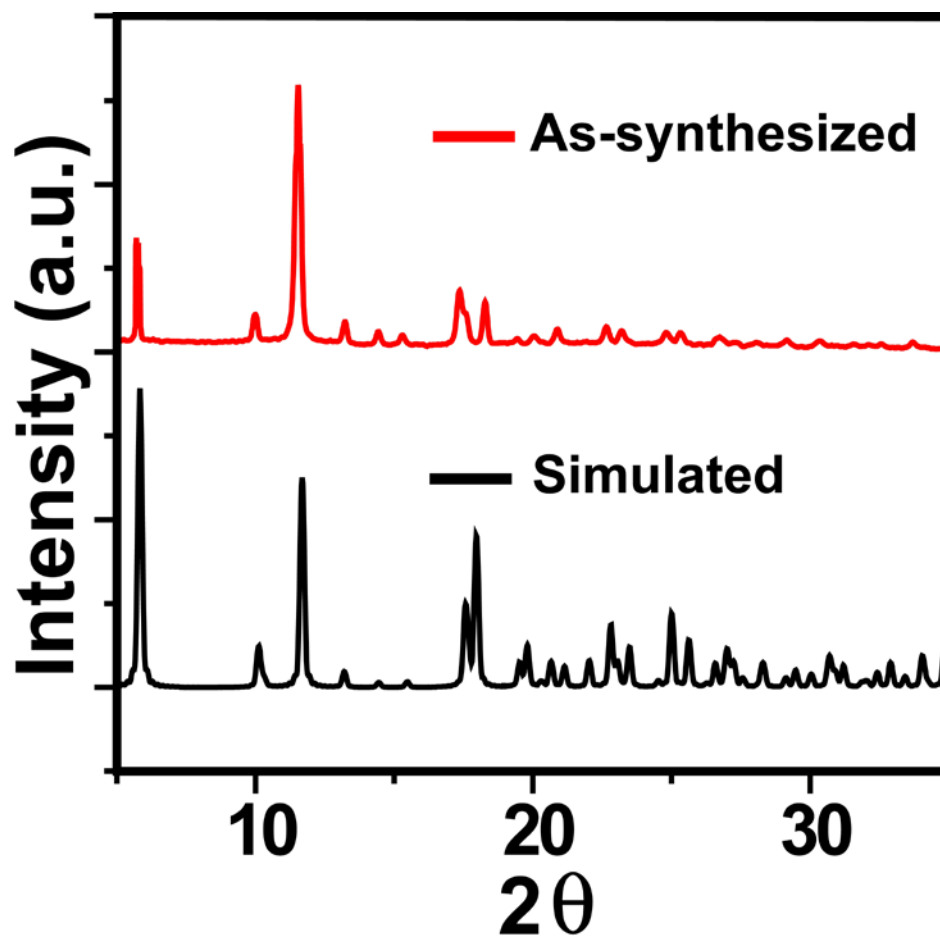


Figure S3. Experimental PXRD pattern of ThrZnOAc compared with the simulated one, exhibiting phase purity of the bulk material.

Section S2. Single crystal X-ray diffraction data collection, structure solution and refinement procedures:

General Data Collection and Refinement Procedures:

Single crystal data were collected on Bruker SMART APEX three circle diffractometer equipped with a CCD area detector and operated at 1500 W power (50 kV, 30 mA) to generate Mo K α radiation ($\lambda=0.71073$ Å). The incident X-ray beam was focused and monochromated using Bruker Excalibur Gobel mirror optics. Crystals of all MOFs reported in the paper was mounted on nylon CryoLoop (Hampton Research) with Paraton-N (Hampton Research).

Initial scans of each specimen were performed to obtain preliminary unit cell parameters and to assess the mosaicity (breadth of spots between frames) of the crystal to select the required frame width for data collection. In every case frame widths of 0.5° were judged to be appropriate and full hemispheres of data were collected using the *Bruker SMART*¹ software suite. Following data collection, reflections were sampled from all regions of the Ewald sphere to redetermine unit cell parameters for data integration and to check for rotational twinning using *CELL_NOW*². In no data collection was evidence for crystal decay encountered. Following exhaustive review of the collected frames the resolution of the dataset was judged. Data were integrated using Bruker *SAINT*³ software with a narrow frame algorithm and a 0.400 fractional lower limit of average intensity. Data were subsequently corrected for absorption by the program *SADABS*⁴. The space group determinations and tests for merohedral twinning were carried out using *XPREP*⁵. In these cases, the highest possible space group was chosen.

Structure was solved by direct method and refined using the *SHELXTL 97*⁵ software suite. Atoms were located from iterative examination of difference F-maps following least squares refinements of the earlier models. Final model was refined anisotropically (if the number of data permitted) until full convergence was achieved. Hydrogen atoms were placed in calculated positions (C-H = 0.93 Å) and included as riding atoms with isotropic displacement parameters 1.2-1.5 times U_{eq} of the attached C atoms. Modeling of solvent water molecules became difficult due to dynamic nature of oxygen and hydrogen molecules within the large pores of the framework. Increasing the exposure time of the crystal

to X-rays did not improve the quality of the high angle data in these cases, as the intensity from low angle data saturated the detector and minimal improvement in the high angle data was achieved. Additionally, diffuse scattering from the highly disordered solvent within the void spaces of the framework and from the capillary to mount the crystal contributes to the background and the 'washing out' of the weaker data. Unfortunately, larger crystals, which would usually improve the quality of the data, presented a lowered degree of crystallinity and attempts to optimize the crystal growing conditions for large high-quality specimens have not yet been fruitful. Single Crystal X-ray Diffraction data was collected at 100(2) K if otherwise stated. Structure was examined using the *ADDSYM* subroutine of *PLATON*⁷ to assure that no additional symmetry could be applied to the models. All ellipsoids in *ORTEP* diagrams are displayed at the 50% probability level. Elevated R-values are commonly encountered for the reasons expressed above by some research groups.⁸⁻¹⁷

1. Bruker (2005). *APEX2*. Version 5.053. Bruker AXS Inc., Madison, Wisconsin, USA.
2. a) G. M. Sheldrick, (2004). *CELL_NOW*. University of Göttingen, Germany. b) T. Steiner, *Acta Cryst.* **1998**, *B54*, 456–463.
3. Bruker (2004). *SAINT-Plus* (Version 7.03). Bruker AXS Inc., Madison, Wisconsin, USA.
4. G. M. Sheldrick, (2002). *SADABS* (Version 2.03) and *TWINABS* (Version 1.02). University of Göttingen, Germany.
5. G. M. Sheldrick, (1997). *SHELXS '97* and *SHELXL '97*. University of Göttingen, Germany.
6. L. J. Farrugia, *J. Appl. Cryst.* **1999**, *32*, 837-838.
7. A. L. Spek (2005) *PLATON, A Multipurpose Crystallographic Tool*, Utrecht University, Utrecht, The Netherlands.
8. L. A. Dakin, P. C. Ong, J. S. Panek, R. J. Staples, P. Stavropoulos, *Organometallics* **2000**, *19*, 2896-2908.
9. S. Noro, R. Kitaura, M. Kondo, S. Kitagawa, T. Ishii, H. Matsuzaka, M. Yamashita, *J. Am. Chem. Soc.* **2002**, *124*, 2568-2583.

10. M. Eddaoudi, J. Kim, D. Vodak, A. Sudik, J. Wachter, M. O’Keeffe, O. M. Yaghi, *Proc. Natl. Acad. Sci. U.S.A.* **2002**, *99*, 4900-4904.
11. R. A. Heintz, H. Zhao, X. Ouyang, G. Grandinetti, J. Cowen, K. R. Dunbar, *Inorg. Chem.* **1999**, *38*, 144-156.
12. K. Biradha, , Y. Hongo, M. Fujita, *Angew. Chem. Int. Ed.* **2000**, *39*, 3843-3845.
13. P. Grosshans, A. Jouaiti, M. W. Hosseini, N. Kyritsakas, *New J. Chem, (Nouv. J. Chim,)* **2003**, *27*, 793-797.
14. N. Takeda, K. Umemoto, K. Yamaguchi, M. Fujita, *Nature (London)* **1999**, *398*, 794-796.
15. M. Eddaoudi, J. Kim, N. Rosi, D. Vodak, J. Wachter, M. O’Keeffe, O. M. Yaghi, *Science* **2002**, *295*, 469-472.
16. B. Kesanli, Y. Cui, M. R. Smith, E. W. Bittner, B. C. Bockrath, W. Lin, *Angew. Chem. Int. Ed.* **2005**, *44*, 72-75.
17. F. A. Cotton, C. Lin, C. A. Murillo, *Inorg. Chem.* **2001**, *40*, 478-484.

Experimental and Refinement Details for MOF:

Colorless rod shaped crystal ($0.60 \times 0.20 \times 0.20 \text{ mm}^3$) was mounted on 0.7 mm diameter nylon CryoLoops (Hampton Research) with Paraton-N (Hampton Research). The loop was mounted on a SMART APEX three circle diffractometer equipped with a CCD area detector (Bruker Systems Inc., 1999a)¹⁹ and operated at 1500 W power (50 kV, 30 mA) to generate Mo K_{α} radiation ($\lambda=0.71073 \text{ \AA}$). The incident X-ray beam was focused and monochromated using Bruker Excalibur Gobel mirror optics. Analysis of the data showed negligible decay during collection. The structure was solved in the hexagonal $P6_1$ space group, with $Z = 6$, using direct method. All non-hydrogen atoms were refined anisotropically. Very high displacement parameters, high esd’s and partial occupancy due to the disorder make it impossible to determine accurate positions for the hydrogen atoms in water molecules. Crystallographic data (excluding structure factors) for the structures are reported in this paper have been deposited with the CCDC as deposition No.CCDC 943050.

Table S1. Crystal Data and Structure Refinement for the MOF (100K).

Identification code	ThrZnOAc	
Empirical formula	$C_{12}H_{26}N_2O_{10}Zn$	
Formula weight	423.66	
Temperature	100(2) K	
Wavelength	0.71073 Å	
Crystal system	Hexagonal	
Space group	P61	
Unit cell dimensions	a = 17.4807(3) Å	$\alpha = 90^\circ$.
	b = 17.4807(3) Å	$\beta = 90^\circ$.
	c = 10.4350(2) Å	$\gamma = 120^\circ$.
Volume	2761.47(9) Å ³	
Z	6	
Density (calculated)	1.492 Mg/m ³	
Absorption coefficient	1.385 mm ⁻¹	
F(000)	1272.0	
Crystal size	0.6 x 0.2 x 0.2 mm ³	
Theta range for data collection	3.04 to 28.06°.	
Index ranges	-22 ≤ h ≤ 22, -23 ≤ k ≤ 22, -13 ≤ l ≤ 12	
Reflections collected	7339	
Independent reflections	3035 [R(int) = 0.0263]	
Completeness to theta = 25.00°	99.8 %	
Absorption correction	Semi-empirical from equivalents	
Max. and min. transmission	0.758 and 0.724	
Refinement method	Full-matrix least-squares on F ²	
Goodness-of-fit on F ²	1.05	
Final R indices [I > 2σ(I)]	R1 = 0.0513, wR2 = 0.1358	
R indices (all data)	R1 = 0.0533, wR2 = 0.1378	
Absolute structure parameter	0.0 (9)	
Largest diff. peak and hole	1.305 and -0.611 e.Å ⁻³	

Ortep Figure

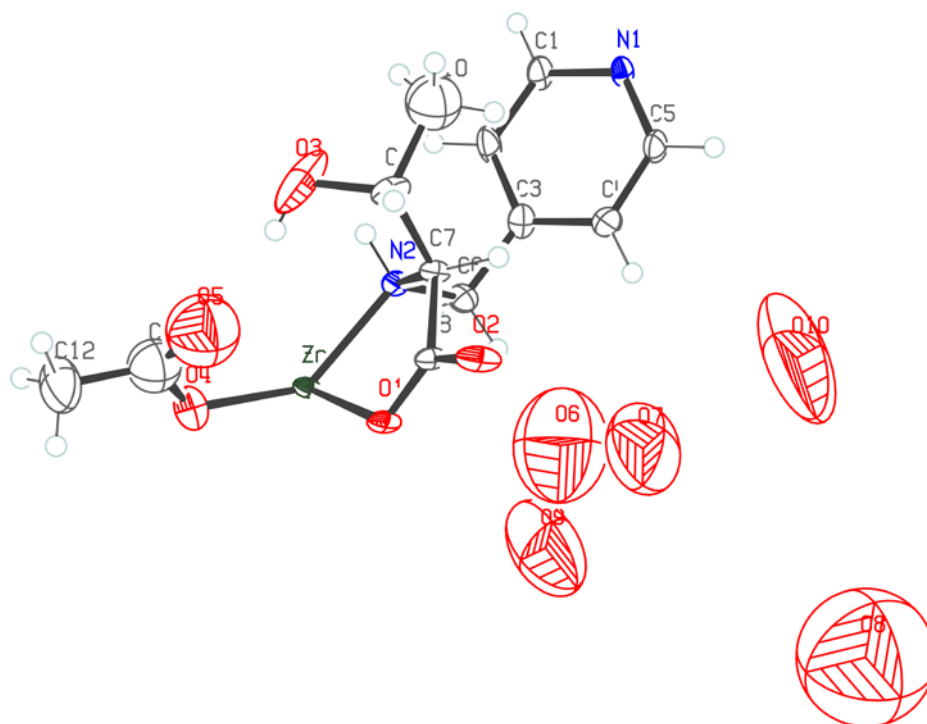


Figure S4. ORTEP diagram of the asymmetric unit of ThrZnOAc. All ellipsoids in *ORTEP* diagrams are displayed at the 50% probability level.

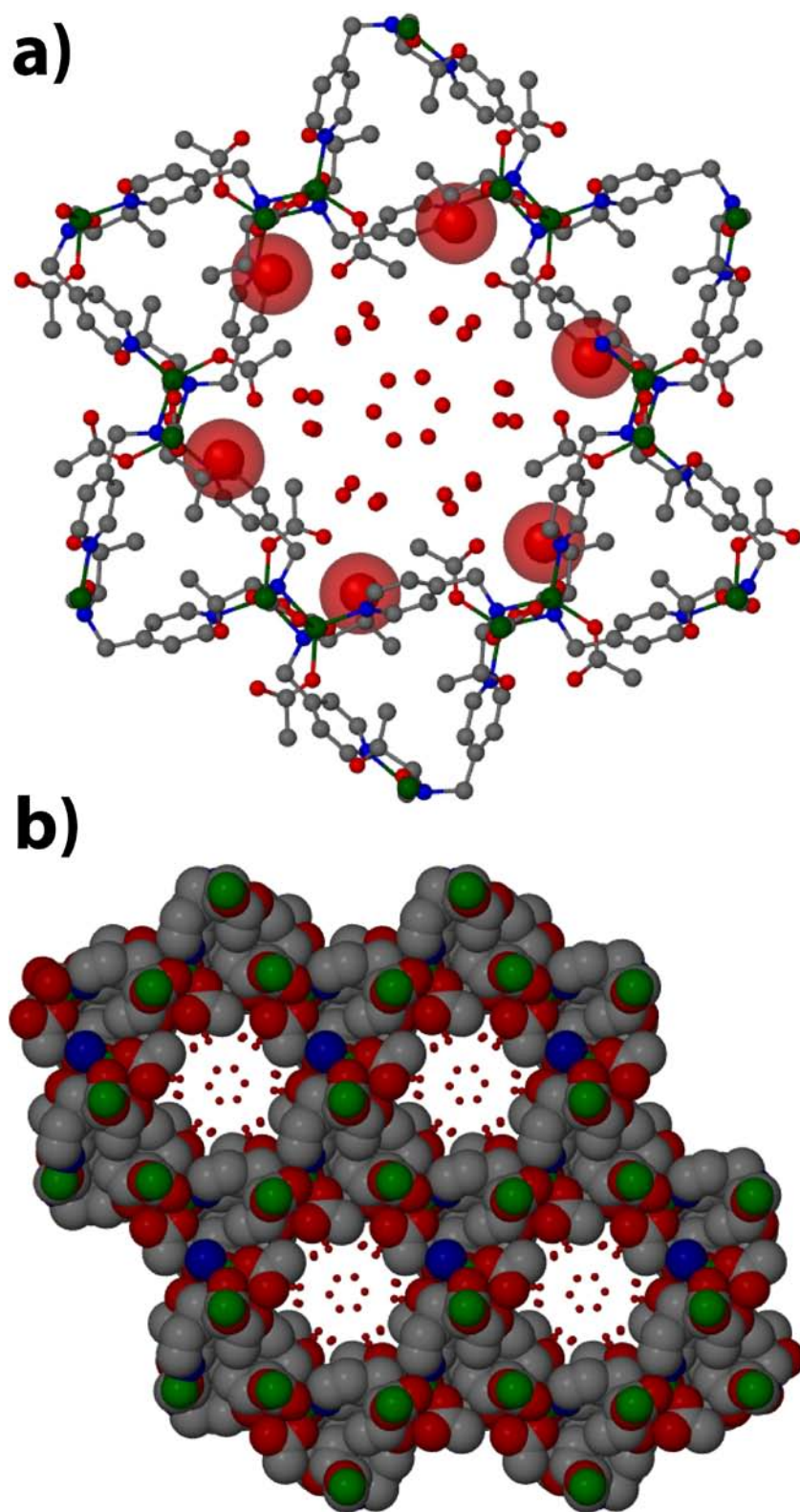


Figure S5. Packing view of ThrZnOAc a) single pore with hydroxy group in spacefill mode. b) Spacefill model of the ThrZnOAc featuring four pore.

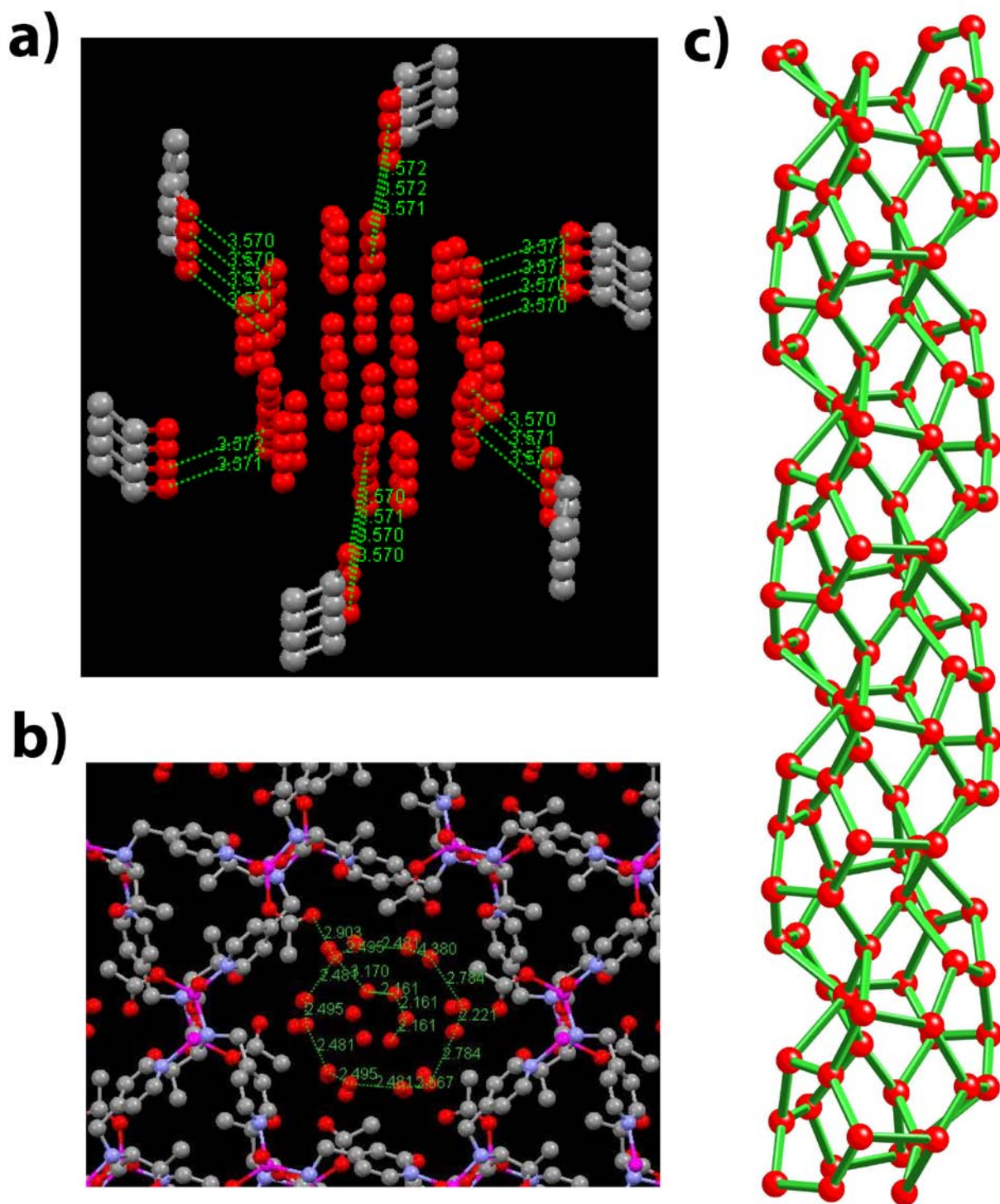


Figure S6. a) A snapshot of the hydrogen bonding interaction between the hydroxy group of the hydroxyethyl sidearm and the solvent water molecules (3.57 Å) along the pore. b) two dimensional view of the intermolecular hydrogen bonding interaction between the solvent water molecules inside the pore featuring high hydrophilic pore surface in case of ThrZnOAc. c) three dimensional hydrogen bonded water molecules arranged as continuous cluster along the pore of ThrZnOAc.

Section S3. Variable Temperature Variable Temperature Powder X-Ray Diffraction study (VT-PXRD) on ThrZnOAc:

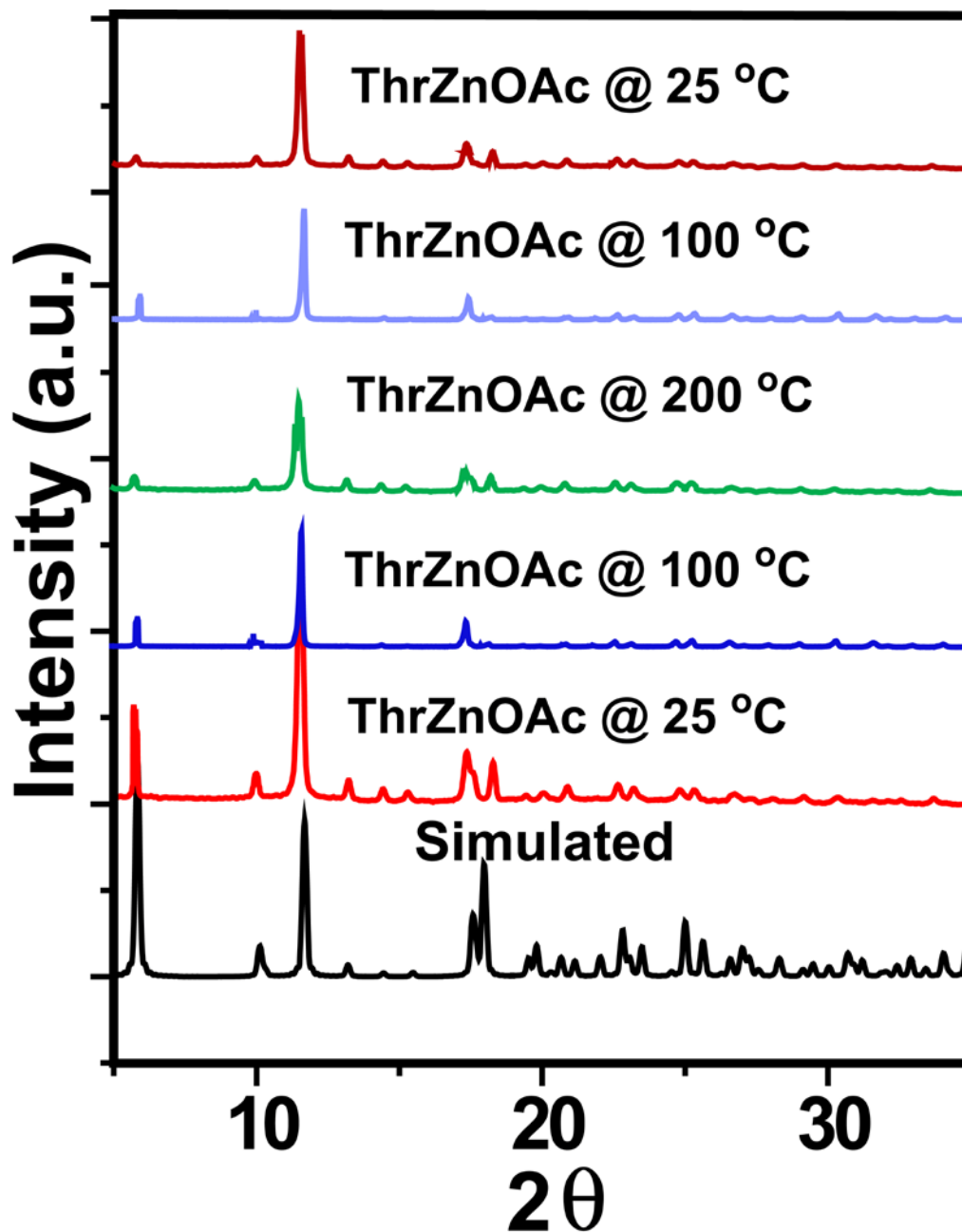


Figure S7: VTPXRD pattern of ThrZnOAc operating from RT to 200 °C and compared with the simulated one showing architectural stability as well as retention of crystallinity even at high temperature range (~200 °C).

Section S4. TGA data and the thermal stability of the ThrZnOAc.

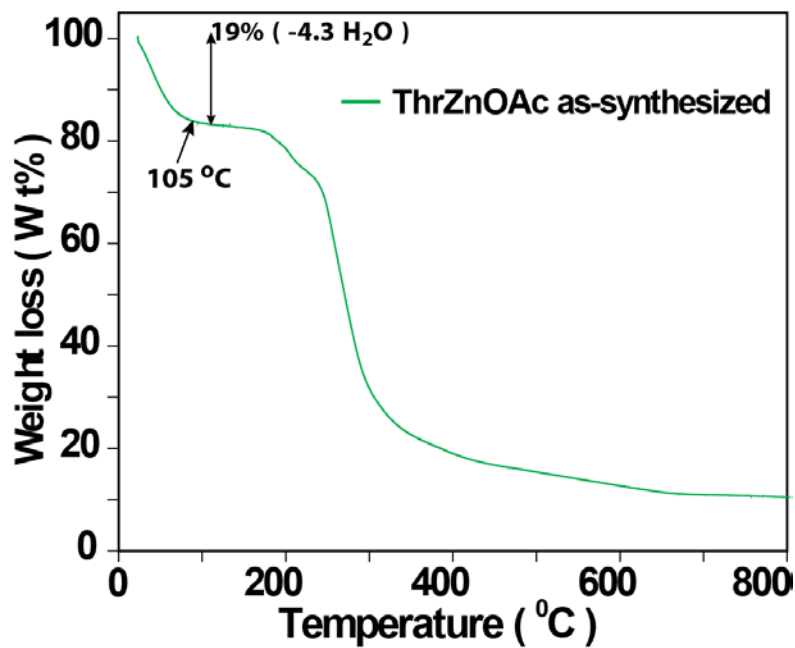


Figure S8: Thermogravimetric analysis of ThrZnOAc showcasing thermal stability upto 210 °C.